Enhancement of the Secondary-Electron Production Process in Front of Insulator Surfaces

Kenji Kimura,* Gou Andou, and Kaoru Nakajima

Department of Engineering Physics and Mechanics, Kyoto University, Kyoto 606-8501, Japan

(Received 10 August 1998)

The secondary-electron yield induced by 0.5-MeV protons specularly reflected from KCl(001) is measured. The observed yield is about 160 electrons/proton at a glancing incidence angle $\theta_i = 1$ mrad and decreases to 100 electrons/proton with increasing θ_i up to 7 mrad, which is about 4 times larger than that for a semiconductor SnTe(001) surface. The enhancement can be ascribed to an almost complete conversion efficiency of excited surface plasmons into electron-hole pairs and a large band gap which results in the efficient production of secondary electrons by the single-electron excitation process. [S0031-9007(98)07931-9]

PACS numbers: 79.20.Rf, 34.50.Dy, 61.82.Ms

Electron emission is a ubiquitous phenomenon in particle-solid interaction and is of great importance in many applications, for example, in particle detectors, in plasma-wall interactions, and in surface analysis techniques, such as ion microscopy and scanning electron microscopy. Investigations have been focused on the electron emission from metals and semiconductors so far [1]. The electron emission from insulators is an intriguing phenomenon from a viewpoint of both fundamental physics and application. Nevertheless, there have been a relatively small number of studies because of the difficulty arising from surface charging during the ion bombardment. Careful investigations revealed that the yield of kinetic electron emission (KEE) is much larger for insulators than for metals and semiconductors [2–6]. This was attributed to a larger electron escape depth due to reduced electron scattering and to a lower surface barrier which results in a larger escape probability through the surface for excited electrons in insulators than in metals and semiconductors. The excitation process in insulators was usually assumed to be suppressed due to the large band gap [6]. However, there is no clear evidence to support this assumption.

Recently, electron emission from insulators at impact of slow highly charge ions has been extensively studied [7,8]. It was suggested that potential electron emission (PEE) by highly charged ions is suppressed in front of a LiF(001) surface rather than in front of metal surfaces, although the less efficient above surface electron emission is more than compensated for by being more efficient below the surface emission from LiF(001), resulting in higher electron yields from LiF than from a Au target for the impact of slow highly charged ions [7].

In a previous study, we have shown that the excitation process can be studied separately from other processes (transportation to the surface and transmission through the surface barrier) utilizing the specular reflection of fast ions at single crystal surfaces [9]. In contrast to a phenomenological theory [10], it was found that the excitation rate is not proportional to the stopping power. In the present Letter, we employ the same technique to address the secondary-electron production process at insulator surfaces. It is demonstrated for the first time that the KEE process is enhanced in front of the insulator surface rather than the semiconductor surface. The origin of the observed enhancement is discussed.

Single crystals of KCl and LiF (7 mm in length along the beam direction and 20 mm in the vertical direction) cleaved along (001) in the air were mounted on a five-axis precision goniometer in an ion-pumped UHV chamber (base pressure 3×10^{-10} Torr). The surfaces were kept at 250 °C under UHV conditions to prepare clean surfaces [11]. The elevated temperature also allowed us to avoid the surface charging by ionic conduction. A beam of 0.5-MeV protons from the 1.7-MV Tandetron accelerator of Kyoto University was collimated by a series of apertures to less than 0.1×0.1 mm^2 and to a divergence angle less than 0.3 mrad. The beam was incident on the target surfaces at a glancing angle. The azimuthal angle of the crystal was carefully chosen to avoid surface axial channeling. A typical intensity of the proton beam was as low as ~1000 ions/s, which guaranteed no macroscopic charging and the negligible radiation damage during the measurement.

When the angle θ_i of incidence measured from the surface plane is smaller than a critical angle [7.7 mrad for the 0.5-MeV proton on KCl(001)], the proton is reflected at a specular angle without penetration inside the crystal [12,13]. The proton may produce secondary electrons outside the crystal during the reflection. These electrons are not subject to the transport and transmission processes. This allows one to measure the production process separately from other processes.

The protons scattered at the specular angle were selected by an aperture ($\phi = 1$ mm) placed 425 mm downstream from the target and were detected by a silicon surface barrier detector. Secondary electrons emitted from the target crystal were detected by a microchannel plate (MCP, effective diameter $\phi = 20$ mm) placed at 9 mm in front of the target. The pulse height of the MCP signal is proportional to the number of secondary electrons detected [8]. The MCP was biased at +500 V

 0031-9007/98/81(24)/5438(4)$15.00

to collect all secondary electrons emitted from the target. The applied bias caused a small deflection of the ion beam, which was estimated to be less than 0.3 mrad under the present experimental conditions.

Figure 1 displays an example of the pulse height distribution of the MCP signal measured in coincidence with the 0.5-MeV proton specularly reflected from KCl(001) at $\theta_i = 2.5$ mrad. The open circles show the pulse height distribution observed without the proton beam (the abscissa is elongated by a factor of 5). These signals are attributed to the free electrons inside the chamber created by the ion pump, and the distribution can be decomposed into two Gaussians. The peak positions I_1 and I_2 of the Gaussians have a relation $I_2 = 2I_1$ indicating that these Gaussians correspond to signals of single- and double-electron detections. The secondary-electron yield can be given by $\gamma = \langle I \rangle / (\varepsilon I_1)$, where $\langle I \rangle$ denotes the mean value of the pulse height distribution, and ε is the efficiency of the MCP, which was measured to be 0.6 for 0.5-keV electrons [14].

Figure 2 depicts the temperature dependence of the observed secondary-electron yield when 0.5-MeV protons were incident on the LiF(001) surface at $\theta_i = 4.1$ mrad. The secondary-electron yield from insulators at normal incidence is known to decrease with temperature due to increasing electron-phonon interaction [6,10]. The present result does not show any temperature dependence at $T > 50\,^{\circ}\mathrm{C}$, indicating that the observed secondary electrons were produced outside the crystal surface. The rapid decrease below $T = 50\,^{\circ}\mathrm{C}$ is ascribed to the macroscopic surface charging.

Figure 3 shows the secondary-electron yield from KCl(001) induced by the 0.5-MeV proton as a function of θ_i together with the secondary-electron yield from a semiconductor SnTe(001) surface measured in a previous paper [9]. Both KCl and SnTe have the same crystal structure (NaCl-type) with almost the same lattice constant (the difference is less than 0.5%). The secondary-electron yield is about 4 times larger for KCl than for SnTe, although the large band gap suggests the reduction for KCl [6]. The observed energy losses $\Delta E(\theta_i)$ of the reflected protons for KCl(001) and SnTe(001) surfaces are also shown for comparison [$\Delta E(\theta_i)$ for SnTe(001) is reproduced from Ref. [15]]. While the secondary-electron yields show a large difference between KCl and SnTe, the energy losses are almost the same. The energy loss of the proton per one electron emission for KCl is about 40 eV/electron at $\theta_i = 7$ mrad, and it decreases down to 20 eV/electron with decreasing θ_i. Recalling that the binding energy of the valence band (Cl $3p$ band) is 9–11 eV and the bulk plasmon energy is 14 eV for KCl [16], the obtained value of 20 eV/electron is surprisingly small. Similar results were obtained with LiF(001), showing that the enhancement of the secondary-electron yield is a common feature for insulator surfaces.

More detailed information is extracted from the data to understand the present result. We have shown that the position-dependent secondary-electron production rate $P(x)$, i.e., the number of secondary electrons produced by a proton per unit path length traveling parallel to the surface at a distance x from the surface, can be derived from the observed $\gamma(\theta_i)$,

$$P(x) = -\frac{1}{2\pi E}\frac{dV(x)}{dx} \times \left(\gamma(0)\sqrt{\frac{E}{V(x)}} + \int_0^{\pi/2} \frac{d\gamma(\theta_i)}{d\theta_i}\bigg|_{\theta_i = \sqrt{V(x)/E}\,\sin(u)} du \right), \quad (1)$$

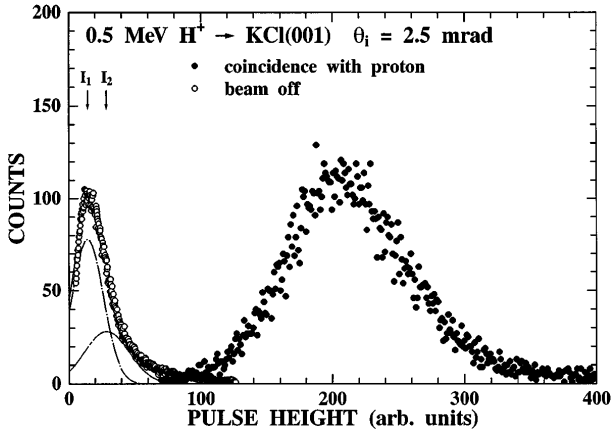

FIG. 1. Pulse height distribution of secondary electrons detected by MCP in coincidence with the 0.5-MeV protons specularly reflected from KCl(001) at $\theta_i = 2.5$ mrad. The open circles show the pulse height distribution measured without the proton beam (the abscissa is elongated by a factor of 5), which corresponds to the signals of single- and double-electron detection.

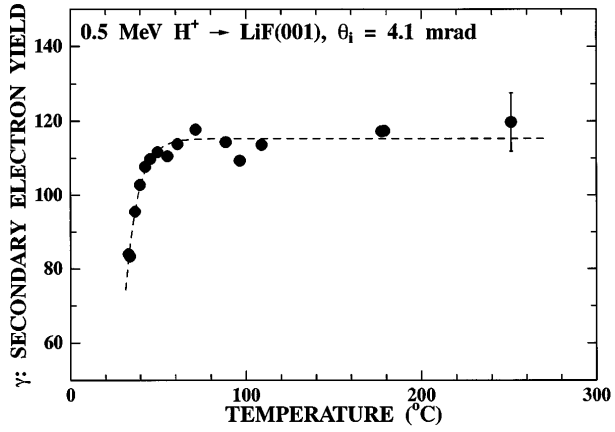

FIG. 2. Secondary-electron yield induced by 0.5-MeV proton specularly reflected from a LiF(001) at $\theta_i = 4.1$ mrad as a function of temperature. The rapid decrease at $T < 50\,^{\circ}\mathrm{C}$ is due to the macroscopic surface charging. A typical experimental error is shown.

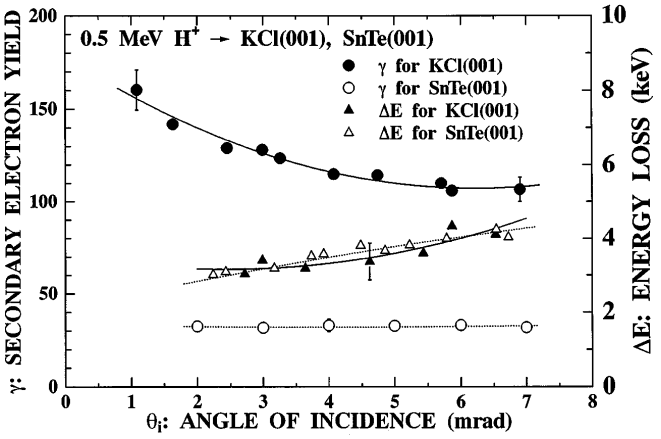

FIG. 3. Secondary-electron yield induced by 0.5-MeV protons specularly reflected from a KCl(001) as a function of θ_i. The result for a SnTe(001) from the Ref. [9] is also shown by open circles. Energy losses of the reflected protons at KCl(001) (closed triangles) and SnTe(001) (open triangles, from Ref. [15]) are shown for comparison. Typical experimental errors are shown.

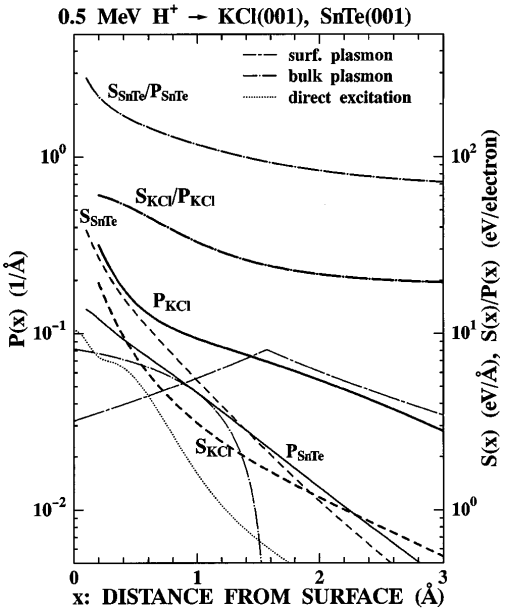

FIG. 4. Position-dependent secondary-electron production rate $P(x)$ for the 0.5-MeV proton at KCl(001) surface (thick solid curve) together with the surface stopping power $S(x)$ (thick dashed curve). The ratio of $S(x)/P(x)$ is shown by a dot-dashed curve. Production rate, stopping power, and the ratio $S(x)/P(x)$ for SnTe(001) (from Ref. [9]) are shown for comparison by thin curves. Calculated results of direct excitation rate and excitation rates of bulk and surface plasmons are also shown.

where E is the proton energy and $V(x)$ the surface continuum potential [9]. The obtained result for 0.5-MeV proton at KCl(001) is displayed together with the previous result for SnTe(001) in Fig. 4 (thick and thin solid curves). The production rate for KCl(001) is larger than SnTe(001) especially at large x.

The position-dependent stopping power $S(x)$ can also be derived from the observed energy loss using a similar equation to Eq. (1) by replacing $P(x)$ and $\gamma(\theta_i)$ with $S(x)$ and $\Delta E(\theta_i)$, respectively. The result of the stopping power for KCl(001) is shown by a thick dashed curve in Fig. 4. Both the production rate and the stopping power decrease with x, but the stopping power decreases more rapidly. The ratio $S(x)/P(x)$, which is assumed to be constant in the phenomenological theory [2], is shown by a thick dot-dashed curve. The ratio is about 60 eV/electron at $x \sim 0$, decreases with x, and becomes almost constant $\sim$20 eV/electron at $x > 2$ Å.

The position-dependent secondary-electron production rate by MeV protons at SnTe(001) was quantitatively explained by the direct electron excitation and the decay of the excited bulk and surface plasmons into electron-hole pairs [9]. The probabilities of the direct excitation and the plasmon excitation were calculated with a binary encounter model and a model given by Kawai *et al.* [17], respectively. The calculated results for the 0.5-MeV proton at KCl(001) are shown by thin curves in Fig. 4. In the calculation, the bulk plasmon energy $\hbar\omega_p = 14$ eV [16] was used, and the electronic surface was assumed to be outside of the atomic surface by half of the interplanar separation (3.15 Å/2). It can be seen that the contribution of the surface plasmon excitation is dominant outside of the electronic surface. In this region, the observed ratio $S(x)/P(x)$ is almost constant, i.e., $\sim$20 eV/electron which is about twice the surface plasmon energy $\hbar\omega_s = 10$ eV. This implies that all surface plasmons decay into electron-hole pairs and half of the excited electrons appears as secondary electrons, while the other half of electrons is impinged inside the crystal. The surface plasmon can decay via photon emission when the momentum-conservation law is violated by surface roughness [18]. The probability of the surface plasmon decay to an electron-hole pair was estimated to be 30% at SnTe(001) [9] and $\leq$30% at Al surfaces [19]. The present large conversion probability at KCl(001) is ascribed to the flatness of the cleaved surface. Observation by atomic force microscopy revealed that the cleaved KCl(001) surface was atomically flat, whereas the SnTe(001) surface had many surface steps introduced during the preparation [20].

With decreasing x, the contribution of the surface plasmon decreases, and the direct excitation process and the bulk plasmon process become dominant. While no large difference is expected in the bulk plasmon process because the bulk plasmon energies of KCl (14 eV) and SnTe (15 eV) are almost the same, the large band gap in KCl suggests a suppression of the direct excitation process [6]. The stopping power of the KCl(001) surface is, indeed, smaller than SnTe(001) at $x < 1.9$ Å in accordance with the above discussion. The secondary-electron production rate for KCl is, however, enhanced almost twice that for SnTe. Consequently, the ratio

$S(x)/P(x)$ for KCl is more than 3 times larger than SnTe. This can be attributed to neither the large mean free path nor the large escape probability for KCl, since the observed secondary electrons are produced outside the crystal surface. A possible explanation might be related to the large band gap in KCl. The forbidden band extended from the Cl $3p$ band (-9 eV) up to the bottom of the conduction band which locates just below the vacuum level (-0.4 eV). There are a relatively small number of the excited states below the vacuum level. Thus the energy lost by the proton is efficiently used to produce free electrons over the vacuum level at KCl(001). Quantitative explanation is left for theoretical study.

In summary, we have demonstrated clear evidence of the enhancement of the secondary-electron production process at insulator surfaces. This indicates that not only the transport and transmission processes but also the production process itself are enhanced for KEE in insulators rather than semiconductors or metals. This is opposite the finding for PEE at the impact of slow highly charged ions on insulator surfaces.

We are grateful to Professor Imanishi and other members of the Department of Nuclear Engineering at Kyoto University for the use of the Tandetron accelerator.

*Author to whom correspondence should be addressed. FAX: +81-75-753-5253.
Electronic address: kimura@kues.kyoto-u.ac.jp

[1] See, for example, M. Rösler and W. Brauer, in *Particle Induced Electron Emission I*, edited by G. Hohler and E. A. Niekisch, Springer Tracts in Modern Physics Vol. 122 (Springer-Verlag, Heidelberg, 1991), p. 1.
[2] C. Baboux, M. Perdrix, R. Goutte, and C. Guilland, J. Phys. D **4**, 1617 (1971).
[3] W. Krönig, K. H. Krebs, and S. Rogashewski, Int. J. Mass Spectrom. Ion Phys. **16**, 243 (1975).
[4] L. A. Alonso, R. A. Baragiola, J. Ferron, and A. Oliva-Florio, Radiat. Eff. **45**, 119 (1979).
[5] H. Jacobsson and G. Holmén, Phys. Rev. B **49**, 1789 (1994).
[6] J. Schou, in *Ionization of Solids by Heavy Particles*, edited by R. A. Baragiola (Plenum, New York, 1993), p. 351.
[7] HP. Winter, M. Vana, C. Lemell, and F. Aumayer, Nucl. Instrum. Methods Phys. Res., Sect. B **115**, 224 (1996).
[8] T. Schenkel, A. V. Barnes, M. A. Briere, A. Hamza, A. Schach von Wittenau, and D. H. Schneider, Nucl. Instrum. Methods Phys. Res., Sect. B **125**, 153 (1997).
[9] K. Kimura, S. Ooki, G. Andou, K. Nakajima, and M. Mannami, Phys. Rev. A **58**, 1282 (1998).
[10] See, for example, D. Hasselkamp, in *Particle Induced Electron Emission II* edited by G. Hohler and E. A. Niekisch, Springer Tracts in Modern Physics Vol. 123 (Springer-Verlag, Heidelberg, 1991), p. 1.
[11] M. Prutton, *Surface Physics* (Clarendon, Oxford, 1983), p. 9.
[12] G. S. Harbinson, B. W. Farmery, H. J. Pabst, and M. W. Thompson, Radiat. Eff. **27**, 97 (1975).
[13] K. Kimura, M. Hasegawa, Y. Fujii, M. Susuki, and M. Mannami, Nucl. Instrum. Methods Phys. Res., Sect. B **33**, 358 (1988).
[14] M. Galanti, R. Gott, and J. F. Renaud, Rev. Sci. Instrum. **42**, 818 (1971).
[15] K. Kimura, H. Kuroda, M. Fritz, and M. Mannami, Nucl. Instrum. Methods Phys. Res., Sect. B **100**, 356 (1995).
[16] A. Akkerman, A. Breskin, R. Chechik, and A. Gibrekhterman, in *Ionization of Solids by Heavy Particles* (Ref. [6]), p. 359; L. Marton and L. B. Leder, Phys. Rev. **94**, 203 (1954).
[17] R. Kawai, N. Itoh, and Y. H. Ohtsuki, Surf. Sci. **114**, 137 (1982).
[18] H. Raether, in *Surface Plasmons on Smooth and Rough Surfaces and on Gratings*, Springer Tracts in Modern Physics Vol. 111 (Springer, Heidelberg, 1988).
[19] J. C. Endritz and W. E. Spicer, Phys. Rev. B **4**, 4159 (1971).
[20] K. Narumi, Y. Fujii, K. Kimura, M. Mannami, and H. Hara, Surf. Sci. **303**, 187 (1994).